

Theory of Thermal Conductivity in High- T_c Superconductors below T_c : Comparison between Hole-Doped and Electron-Doped Systems

Hideyuki HARA and Hiroshi KONTANI

Department of Physics, Nagoya University, Furo-cho, Nagoya 464-8602, Japan.

(Dated: November 1, 2018)

In hole-doped high- T_c superconductors, thermal conductivity κ increases drastically just below T_c , which has been considered as a hallmark of a nodal gap. In contrast, such a coherence peak in κ is not visible in electron-doped compounds, which may indicate a full-gap state such as a $d + is$ -wave state. To settle this problem, we study κ in the Hubbard model using the fluctuation-exchange (FLEX) approximation, which predicts that the nodal d -wave state is realized in both hole-doped and electron-doped compounds. The contrasting behavior of κ in both compounds originates from the differences in the hot/cold spot structure. In general, a prominent coherence peak in κ appears in line-node superconductors *only when the cold spot exists on the nodal line*.

Keywords: spin fluctuation theory, thermal conductivity, unconventional superconductivity, FLEX approximation

In strongly correlated electron systems, transport phenomena give us significant information on the many-body electronic states. In high- T_c superconductors (HTSCs), for example, both the Hall coefficient R_H and the thermoelectric power S are positive in hole-doped compounds such as $\text{YBa}_2\text{Cu}_3\text{O}_{7-\delta}$ (YBCO) and $\text{La}_{2-\delta}\text{Sr}_\delta\text{CuO}_4$ (LSCO), whereas they are negative in electron-doped compounds like $\text{Nd}_{2-\delta}\text{Ce}_\delta\text{CuO}_4$ (NCCO) and $\text{Pr}_{2-\delta}\text{Ce}_\delta\text{CuO}_4$ (PCCO) [1]. These experimental facts originate from the difference in the “cold-spot,” which is the portion of the Fermi surface where the relaxation time of a quasiparticle (QP), $\tau_{\mathbf{k}}$, takes the maximum value [2–4]:

Below T_c , electronic thermal conductivity κ has been observed intensively since it gives us considerable information on the superconducting state; it is the only transport coefficient which remains finite below T_c . For example, the \mathbf{k} -dependence of the SC gap can be determined by the angle resolved measurement of κ under the magnetic field [5, 6]. Also, one can detect the type of nodal gap structure (full-gap, line-node, or point-node) by measuring κ at low temperatures ($T \ll T_c$). For $T \lesssim T_c$, κ also shows rich variety of behavior in various superconductors. In conventional full-gap s -wave superconductors, the opening of the SC gap rapidly decreases the density of thermally excited QPs, causing κ to decrease. On the other hand, κ shows “coherence peak” behavior just below T_c in several unconventional superconductors with line-node gaps, e.g., hole-doped HTSC [7–9], CeCoIn_5 [10, 11], and URu_2Si_2 [12]. A previous theoretical study based on a BCS model with d -wave pairing interaction [13] discussed that the coherence peak in YBCO originates from the steep reduction in τ below T_c .

In sharp contrast, no coherence peak in κ is observed in electron-doped HTSCs [14, 15], irrespective that a recent ARPES measurement [16] suggests that the $d_{x^2-y^2}$ -wave state is realized. The observed \mathbf{k} -dependence of the SC gap function in NCCO, which prominently deviates from $\cos k_x - \cos k_y$, is well reproduced by the

fluctuation-exchange (FLEX) approximation [17], which is a self-consistent spin fluctuation theory. On the other hand, recent point-contact spectroscopy for PCCO [18] suggests that a full-gap SC state such as $d_{x^2-y^2} + is$ or $d_{x^2-y^2} + id_{xy}$ state is realized for $\delta = 0.15$ and 0.17 . To find out the real SC state in electron-doped HTSC, we have to elucidate whether the “absence of coherence peak in κ ” is a crucial hallmark of the full-gap SC state, or it can occur even in nodal gap superconductors.

In this letter, we present a theoretical study of the electronic thermal conductivity κ in HTSCs using the FLEX approximation. This is the first numerical study of transport properties in the SC state based on the repulsive Hubbard model. In deriving the relaxation time $\tau_{\mathbf{k}}$, both the strong inelastic scattering due to Coulomb interaction and weak elastic impurity scattering are taken into consideration, which corresponds to optimally-doped YBCO and NCCO samples, respectively. We find that a sizable coherence peak of κ in YBCO originates from the reduction in inelastic scattering. In contrast, the coherence peak is absent in NCCO in spite of that $d_{x^2-y^2}$ -wave SC state is realized, since the nodal point does not coincide with the cold spot in the normal state. Thus, contrasting behaviors of κ in YBCO and NCCO are explained on the same footing as $d_{x^2-y^2}$ -wave superconductors. This result was not derived in the BCS model [13].

Here, we study the following repulsive Hubbard model:

$$\mathcal{H} = \sum_{\mathbf{k}, \sigma} \epsilon_{\mathbf{k}} c_{\mathbf{k}\sigma}^\dagger c_{\mathbf{k}\sigma} + \frac{U}{N} \sum_{\mathbf{k}, \mathbf{k}'\mathbf{q}} c_{\mathbf{k}+\mathbf{q}\uparrow}^\dagger c_{\mathbf{k}'-\mathbf{q}\downarrow}^\dagger c_{\mathbf{k}'\downarrow} c_{\mathbf{k}\uparrow} \quad (1)$$

where U is the Coulomb interaction and $\epsilon_{\mathbf{k}} = 2t_0(\cos(k_x) + \cos(k_y)) + 4t_1 \cos(k_x) \cos(k_y) + 2t_2(\cos(2k_x) + \cos(2k_y))$ is the kinetic energy of free electrons. Hereafter, we put $t_0 = -1.0$, $t_1 = 0.167$, and $t_2 = -0.2$ [2] to reproduce the Fermi surface of YBCO and NCCO. We also put $U = 8.0$ for YBCO and $U = 5.4$ for NCCO. Here, no phenomenological fitting parameters are introduced except for U .

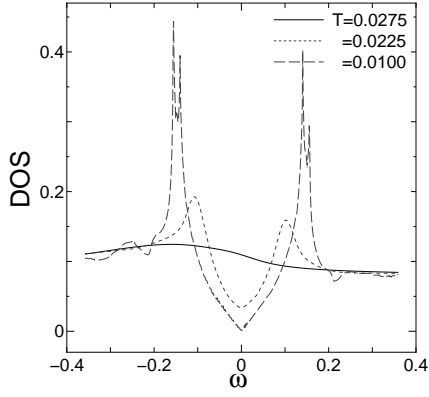


FIG. 1: Temperature dependence of the DOS given by the FLEX approximation for YBCO ($n = 0.9$). Note that $T_c = 0.024$.

In the FLEX approximation, the normal and anomalous self-energies are given by

$$\Sigma^n(\mathbf{k}, i\epsilon_n) = \frac{U^2 T}{N} \sum_{\mathbf{k}, l} G_{\mathbf{q}+\mathbf{k}}(i\epsilon_n + i\omega_l) \times \left(\frac{3}{2}\chi_s + \frac{1}{2}\chi_c - \chi_0 \right)_{\mathbf{q}, \omega_l} \quad (2)$$

$$\Sigma^a(\mathbf{k}, i\epsilon_n) = \frac{-U^2 T}{N} \sum_{\mathbf{k}, l} F_{\mathbf{q}+\mathbf{k}}^\dagger(i\epsilon_n + i\omega_l) \times \left(\frac{3}{2}\chi_s - \frac{1}{2}\chi_c - \phi_0 \right)_{\mathbf{q}, \omega_l} \quad (3)$$

where $\epsilon_n = \pi T(2n + 1)$ and $\omega_l = 2\pi Tl$ are the Matsubara frequencies for fermions and bosons, respectively. χ_s and χ_c are the dynamical spin and charge susceptibilities, which are given by

$$\chi_s(\mathbf{q}, i\omega_l) = \frac{\chi_0 + \phi_0}{1 - U(\chi_0 + \phi_0)} \quad (4)$$

$$\chi_c(\mathbf{q}, i\omega_l) = \frac{\chi_0 - \phi_0}{1 - U(\chi_0 - \phi_0)} \quad (5)$$

$$\chi_0(\mathbf{q}, i\omega_l) = -\frac{T}{N} \sum_{\mathbf{k}, n} G_{\mathbf{k}+\mathbf{q}}(i\epsilon_n + i\omega_l) G_{\mathbf{k}}(i\epsilon_n) \quad (6)$$

$$\phi_0(\mathbf{q}, i\omega_l) = -\frac{T}{N} \sum_{\mathbf{k}, n} F_{\mathbf{k}+\mathbf{q}}^\dagger(i\epsilon_n + i\omega_l) F_{\mathbf{k}}(i\epsilon_n) \quad (7)$$

where G and F are the normal and anomalous Green function, respectively. They are given by

$$G(i\epsilon_n) = (i\epsilon_n + \tilde{\epsilon}_{\mathbf{k}} + \Sigma^n(-i\epsilon_n))D(i\epsilon_n)^{-1} \quad (8)$$

$$F(i\epsilon_n) = \Sigma^a(-i\epsilon_n)D(i\epsilon_n)^{-1} \quad (9)$$

$$D(i\epsilon_n) = (-\epsilon_n - \tilde{\epsilon}_{\mathbf{k}} + \Sigma^n(-i\epsilon_n))(-\epsilon_n + \tilde{\epsilon}_{\mathbf{k}} + \Sigma^n(i\epsilon_n)) - (\Sigma^a(-i\epsilon_n))^2 \quad (10)$$

where $\tilde{\epsilon}_{\mathbf{k}} = \epsilon_{\mathbf{k}} - \mu$; μ is the chemical potential. In the FLEX approximation, we solve eqs. (2)-(10) self-consistently by choosing μ to adjust the electron filling n .

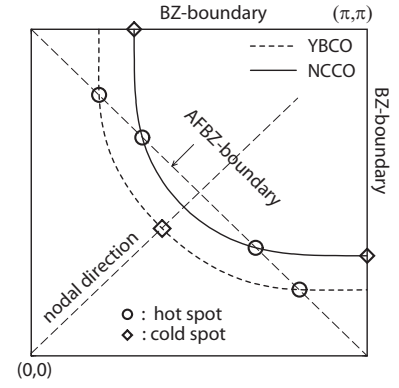


FIG. 2: Position of the hot/cold spots for YBCO ($n = 0.9$) and for NCCO ($n = 1.10$). AFBZ represents the antiferromagnetic Brillouin zone.

In the following numerical study, we use 64×64 \mathbf{k} -meshes and 2048 Matsubara frequencies. Figure 1 represents the density of states (DOS); $\rho(\omega) = \frac{1}{N} \sum_{\mathbf{k}} G_{\mathbf{k}}^A(\omega)/\pi$. Here, the advanced (retarded) Green function $G_{\mathbf{k}}^A(\omega)$ ($G_{\mathbf{k}}^R(\omega)$) is given by the numerical analytic continuation of the Matsubara Green function from the lower (upper) half plane in the complex ω space.

Figure 2 shows the location of the hot/cold spots for both YBCO and NCCO in the normal state. The transport phenomena are governed by QPs around the cold spot, where the QP damping rate $\gamma_{\mathbf{k}} = \text{Im}\Sigma_{\mathbf{k}}^n(-i\delta)$ [$= 1/2\tau_{\mathbf{k}}$] takes the minimum value. According to the FLEX approximation, the cold-spot in hole-doped [electron-doped] systems is around $(\pi/2, \pi/2)$ [$(\pi, 0)$] [2]. The position of the cold-spot in electron-doped systems was confirmed by ARPES measurements [19, 20] after the theoretical prediction [2].

Hereafter, we derive the electric thermal conductivity κ . According to the linear response theory [21–23],

$$\kappa = \frac{-1}{T} \int_0^\beta d\tau \sum_{k_1, k_2} \frac{1}{i\omega} \langle Q_{k_1}(\tau) Q_{k_2}(0) \rangle e^{i\omega\tau} |_{\omega \rightarrow 0} \quad (11)$$

$$\hat{Q}_{\mathbf{k}x}(\tau) = \hat{q}_{\mathbf{k}x\uparrow} + \hat{q}_{\mathbf{k}x\downarrow} + \hat{q}_{\mathbf{k}x}^a + \hat{q}_{\mathbf{k}x}^{a\dagger} \quad (12)$$

where $\hat{Q}_{\mathbf{k}x}$ is the heat current operator in the superconducting state: $\hat{q}_{\mathbf{k}x\sigma}$ and $\hat{q}_{\mathbf{k}x}^a$ are given by

$$\hat{q}_{\mathbf{k}x\sigma} = \omega \hat{v}_{\mathbf{k}x\sigma}, \quad \hat{q}_{\mathbf{k}x}^a = \omega \hat{v}_{\mathbf{k}x}, \quad (13)$$

where $\hat{v}_{\mathbf{k}x\sigma}$ represents the “Fermi velocity” and $\hat{v}_{\mathbf{k}x}^a$ is the “gap velocity” [21]:

$$\hat{v}_{\mathbf{k}x\sigma} = v_{\mathbf{k}x} c_{\mathbf{k}\sigma}^\dagger c_{\mathbf{k}\sigma}, \quad \hat{v}_{\mathbf{k}x}^a = v_{\mathbf{k}x}^a c_{\mathbf{k}\uparrow}^\dagger c_{-\mathbf{k}\downarrow}^\dagger, \quad (14)$$

where $v_{\mathbf{k}x} = v_{\mathbf{k}x}^0 + \frac{\partial \Sigma_{\mathbf{k}}^n}{\partial k_x}$ and $v_{\mathbf{k}x}^a = \frac{\partial \Sigma_{\mathbf{k}}^a}{\partial k_x}$.

As a result, the expression for κ in the SC state with dropping the current vertex correction (CVC) is given by

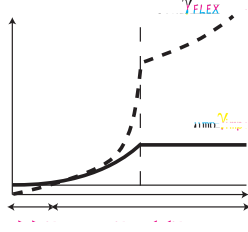


FIG. 3: Schematic T -dependences of $\gamma_{\mathbf{k}}^{\text{FLEX}}$ and γ_{imp} .

[21–23]

$$\begin{aligned} \kappa = & \frac{1}{2T} \sum_{\mathbf{k}} \int dz \left(-\frac{\partial f(z)}{\partial z} \right) \{ 2q_{\mathbf{k}x}^2 (G_{\mathbf{k}}^R(z) G_{\mathbf{k}}^A(z) \\ & - F_{\mathbf{k}}^R(z) F_{\mathbf{k}}^A(z)) \\ & + q_{\mathbf{k}x}^2 (-G_{\mathbf{k}}^R(-z) G_{\mathbf{k}}^R(z) - G_{\mathbf{k}}^A(-z) G_{\mathbf{k}}^A(z)) \\ & + 2F_{\mathbf{k}}^R(z) F_{\mathbf{k}}^A(z) \\ & + 4q_{\mathbf{k}x} q_{\mathbf{k}x}^a (-G_{\mathbf{k}}^R(z) F_{\mathbf{k}}^A(z) - F_{\mathbf{k}}^R(z) G_{\mathbf{k}}^A(z)) \} \quad (15) \end{aligned}$$

where $f(z) = (e^{z/T} + 1)^{-1}$. In the normal state, heat CVC due to Coulomb interaction is small, as shown in the second-order perturbation theory with respect to U [23], and in the FLEX approximation [25]. This fact will also be true below T_c since the particle-nonconserving four point vertex is much smaller than the particle-conserving one [26]. Therefore, we neglect the heat CVC in the present numerical study. We find that the first term in eq. (15), which is proportional to $\{q_{\mathbf{k}x}\}^2$, is predominant, and the other terms which contain the gap velocity, $q_{\mathbf{k}x}^a$, are negligibly small. On the other hand, the charge CVC gives anomalous transport properties for R_H [2], S [3], magnetoresistance [24] and Nernst coefficient [25] both in hole-doped and electron-doped systems. Anomalous transport phenomena due to charge CVC are also observed in CeMIn_5 ($M=\text{Co,Rh}$) [27] and in κ -(BEDT-TTF) $_2\text{X}$ [28].

Here, we include the QP damping due to impurity scattering γ_{imp} by replacing $\Sigma^{nR}(\mathbf{k}, \omega) \rightarrow \Sigma^{nR}(\mathbf{k}, \omega) - i\gamma_{\text{imp}}$. Then, the total QP damping rate is $\gamma_{\mathbf{k}} = \gamma_{\mathbf{k}}^{\text{FLEX}} + \gamma_{\text{imp}}$ [13, 29], where $\gamma_{\mathbf{k}}^{\text{FLEX}} = \text{Im}\Sigma^{nR}(\mathbf{k}, \omega)$. In the t -matrix approximation, $\gamma_{\text{imp}} = n_{\text{imp}} \text{Im}\{-1/(I^{-1} - g_0)\}|_{\omega=0}$, where n_{imp} is the impurity concentration, I is the impurity potential, and $g_0 \equiv \frac{1}{N} \sum_{\mathbf{k}} G_{\mathbf{k}}^R$ is the local Green function. Hereafter, we consider the nearly unitary limit case $I \sim \infty$ where $\gamma_{\text{imp}}(T=0)$ takes a constant value in the self-consistent calculation [13, 29], and assume that $\gamma_{\text{imp}} \ll \gamma_{\mathbf{k}}$ at $T = T_c$. In this case, we are allowed to put $\gamma_{\text{imp}}(T) = \gamma_{\text{imp}}(T=0)$ since the T -dependence of γ_{imp} affects κ near T_c only slightly. A schematic T -dependences of $\gamma_{\mathbf{k}}^{\text{FLEX}}$ and γ_{imp} are shown in Fig. 3.

Figure 4 represents the temperature-dependence of κ given by eq. (15). In YBCO, κ increases drastically below T_c since the AF fluctuations, which are the origin

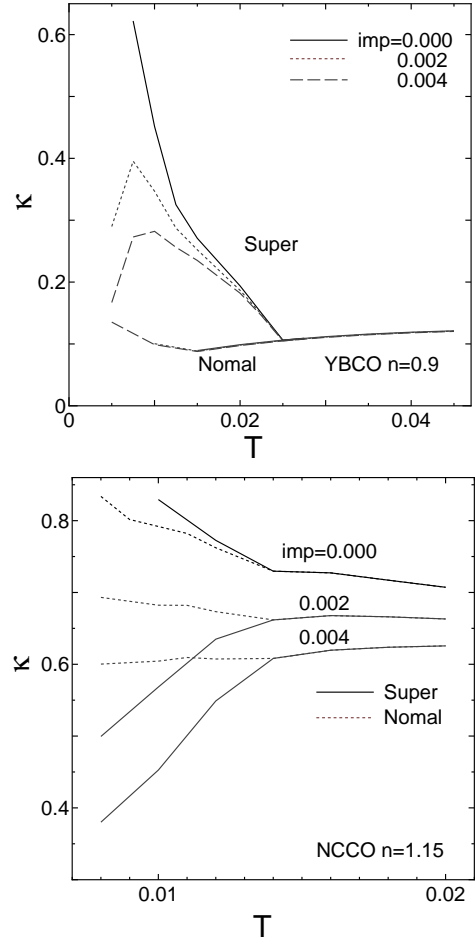


FIG. 4: Obtained κ for YBCO ($n = 0.9$; $T_c = 0.024$) and for NCCO ($n = 1.15$; $T_c = 0.014$), for $\gamma_{\text{imp}} = 0, 0.002$ and 0.004 . “Normal” represents κ given by the normal state FLEX approximation under the constraint $F = \Sigma^a = 0$.

of inelastic scattering, are reduced due to the SC gap. Since $\gamma_{\mathbf{k}}$ is much larger than γ_{imp} at $T > T_c$, κ in the normal state is affected by γ_{imp} only slightly. For $T \ll T_c$, on the other hand, κ is suppressed by γ_{imp} ; κ shows the maximum when $\gamma_{\mathbf{k}}^{\text{FLEX}} \sim \gamma_{\text{imp}}$ is satisfied at the nodal point. The obtained result is consistent with experiments [7–9]. In strong contrast, in NCCO, “coherence peak” in κ is very small even for $\gamma_{\text{imp}} = 0$, which is also consistent with experiments [14, 15].

Here, we discuss the reason why the coherence peak in κ is present in YBCO whereas it is absent in NCCO. Below T_c , only thermally excited QPs above the SC gap can contribute to κ , except at the nodal point. According to eq. (15), thermal conductivities in the normal state (κ_n) and in the line-node SC state (κ_s), where $\rho(\epsilon) \propto |\epsilon|$, are approximately given by

$$\kappa_n \propto T/\gamma_{\text{cold}} \quad (16)$$

$$\kappa_s \propto T^2/\gamma_{\text{node}} \quad (17)$$

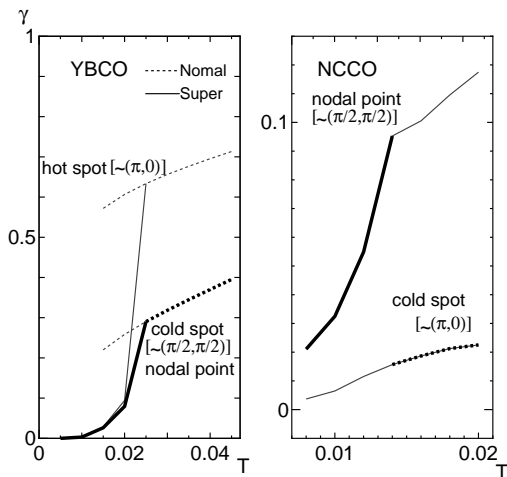


FIG. 5: T -dependence of $\gamma_{\mathbf{k}}$ for both YBCO and NCCO for $\gamma_{\text{imp}} = 0$. Thick full lines and thick broken lines represent γ_{node} ($T < T_c$) and γ_{cold} ($T > T_c$), respectively.

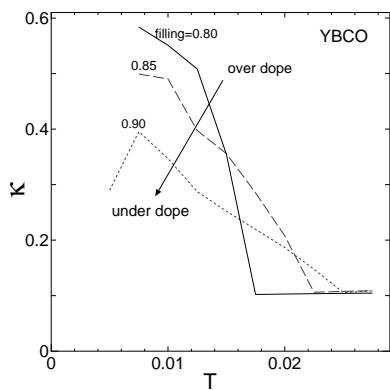


FIG. 6: n -dependence of κ for YBCO; $n = 0.8 \sim 0.9$.

where γ_{cold} and γ_{node} represent $\gamma_{\mathbf{k}}$ at the cold spot above T_c and that at the nodal point below T_c , respectively.

Figure 5 shows the T -dependence of $\gamma_{\mathbf{k}}$ given by the FLEX approximation. In YBCO, both γ_{cold} and γ_{node} are given by $\gamma_{\mathbf{k}}$ at the same point; $\mathbf{k} \approx (\pi/2, \pi/2)$. As the temperature drops, γ_{cold} decreases moderately in proportion to T in the normal state. Below T_c , γ_{node} quickly approaches zero since inelastic scattering is suppressed by the SC gap. As a result, κ shows a prominent coherence peak below T_c , as recognized by eqs. (16) and (17). In NCCO, on the other hand, γ_{cold} is given by $\gamma_{\mathbf{k}}$ at $\mathbf{k} \approx (\pi, 0)$, which is different from the nodal point of the SC gap; $\mathbf{k} \approx (\pi/2, \pi/2)$. Since γ_{node} is much larger than γ_{cold} at $T = T_c$ in NCCO as shown in Fig. 5, κ is not enhanced in NCCO below T_c . Although the numerical accuracy becomes worse for NCCO below $T \sim 0.015$, the obtained result of κ will be qualitatively reliable. In summary, the coherence peak in κ is absent even in nodal SC when the cold spot and the nodal point are different.

Figure 6 shows the obtained doping dependence of κ in

YBCO. In over-doped case ($n = 0.8$), the enhancement of κ is largest, and it decreases in optimally ($n = 0.85$) and under-doped ($n = 0.9$) cases since the cold spot approaches the AFBZ as $n \rightarrow 1$. This tendency is consistent with experiments [7]. Note that in real materials, T_c in under-doped case is smaller than that in optically-doped case. In the FLEX approximation, however, T_c monotonically increases as $n \rightarrow 1$ since the pseudo-gap state in under-doped region cannot be described. The characteristic pseudo-gap phenomena are well described by including the self-energy correction due to strong SC fluctuations into the FLEX approximation, which is called the FLEX+ T -matrix approximation [25, 30].

In the present work, we assumed that the inelastic scattering is dominant, and neglected the temperature dependence of γ_{imp} . This assumption will be allowed for clean optimally-doped HTSCs. In dirty samples where elastic scattering is large, we should calculate the T -dependence of γ_{imp} using the self-consistent t -matrix approximation [13, 29]. In under-doped systems, however, the t -matrix approximation is not sufficient since the radius of “effective impurity potential” is enlarged due to electron-electron correlation, which can be described by the GV^I -method in Ref. [31]. For a reliable study of κ in under-doped systems, it will be necessary to take account of residual disorders using the GV^I -method.

In summary, we studied thermal conductivity κ in HTSCs. In the hole-doped case, κ shows a prominent “coherence peak” below T_c , whereas it is absent in the electron-doped case. Based on the FLEX approximation, such a contrasting behavior of κ is well explained, although both YBCO and NCCO are pure $d_{x^2-y^2}$ -wave superconductors. We do not have to assume a full-gap state in NCCO (such as $d + is$) to explain the absence of a coherence peak, which originates from the fact that the cold spot (line) in the normal state [$\sim (\pi, 0)$] is not on the nodal point (line) of the SC gap. The present study will open the way for the theoretical study of κ in various interesting unconventional superconductors.

The authors acknowledge fruitful discussions with Y. Matsuda and K. Izawa. This work was supported by Grant-in-Aid from MEXT. Numerical calculations were performed at the supercomputer center, ISSP.

-
- [1] J. Takeda, T. Nishikawa, and M. Sato: *Physica C* **231** (1994) 293.
 - [2] H. Kontani, K. Kanki and K. Ueda: *Phys. Rev. B* **59** (1999) 14723.
 - [3] H. Kontani: *J. Phys. Soc. Jpn.* **70** (2001) 2840.
 - [4] H. Kontani and K. Yamada: *J. Phy. Soc. Jpn.* **74** (2005) 155.
 - [5] K. Izawa, H. Yamaguchi, Y. Matsuda, H. Shishido, R. Settai and Y. Onuki: *Phys. Rev. Lett.* **87** (2001) 057002.

- [6] Y. Matsuda, K. Izawa and I. Vekhter, *J. Phys.: Condens. Matter* **18** (2006) R705.
- [7] C.P. Popoviciu and J.L. Cohn: *Phys. Rev. B* **55** (1997) 3155.
- [8] K. Krishana, J. M. Harris, and N. P. Ong: *Phys. Rev. Lett.* **75** (1995) 3529
- [9] Y. Zhang, N. P. Ong, P. W. Anderson, D. A. Bonn, R. Liang, and W. N. Hardy: *Phys. Rev. Lett.* **86** (2001) 890.
- [10] R. Movshovich, M. Jaime, J.D. Thompson¹, C. Petrovic, Z. Fisk, P.G. Pagliuso, and J.L. Sarrao: *Phys. Rev. Lett.* **86** (2001) 5152.
- [11] Y. Kasahara, Y. Nakajima, K. Izawa, Y. Matsuda, K. Behnia, H. Shishido, R. Settai, and Y. Onuki: *Phys. Rev. B* **72** (2005) 214515.
- [12] Y. Matsuda et al, preprint.
- [13] P.J. Hirshfeld and W.O. Putikka: *Phys. Rev. Lett.* **77** (1996) 3909.
- [14] J. L. Cohn, M.S. Osofsky, J.L. Peng, Z. Y. Li, and R.L. Greene: *Phys. Rev. B* **46** (1992) 12053.
- [15] H. Fujishiro, M. Ikeba, M. Yagi, M. Matsukawa, H. Ogasawara and K. Noto: *Physica B* **219&220** (1996) 163.
- [16] H. Matsui, K. Terashima, T. Sato, T. Takahashi, M. Fujita, and K. Yamada: *Phys. Rev. Lett.* **95** (2005) 017003.
- [17] H. Yoshimura and D.S. Hirashima: *J. Phys. Soc. Jpn* **73** (2004) 2057.
- [18] M.M. Qazilbash, A. Biswas, Y. Dagan, R.A. Ott, and R.L. Greene: *Phys. Rev. B* **68** (2003) 024502.
- [19] N.P. Armitage, D.H. Lu, C. Kim, A. Damascelli, K.M. Shen, F. Ronning, D.L. Feng, P. Bogdanov, and Z.-X. Shen: *Phys. Rev. Lett.* **87** (2001) 147003.
- [20] N. P. Armitage, F. Ronning, D. H. Lu, C. Kim, A. Damascelli, K. M. Shen, D. L. Feng, H. Eisaki, Z.-X. Shen, P. K. Mang, N. Kaneko, M. Greven, Y. Onose, Y. Taguchi, and Y. Tokura: *Phys. Rev. Lett.* **88**, 257001 (2002).
- [21] A.C. Durst and P.A. Lee: *Phys. Rev. B* **62** (2000) 1270.
- [22] T. Jujo: *J. Phy. Soc. Jpn.* **70** (2000) 1349.
- [23] H. Kontani, *J. Phys. Rev. B* **67** (2003) 014408.
- [24] H. Kontani: *Phys. Soc. Jpn.* **70** (2001) 1873.
- [25] H. Kontani, *Phys. Rev. Lett.* **89** (2002) 237003.
- [26] A.J. Leggett: *Phys. Rev.* **146** (1965) A1869.
- [27] Y. Nakajima, H. Shishido, H. Nakai, T. Shibauchi, K. Behnia, K. Izawa, M. Hedo, Y. Uwatoko, T. Matsumoto, R. Settai, Y. Onuki, H. Kontani, and Y. Matsuda: *J. Phys. Soc. Jpn.* **76** (2007) 027403.
- [28] K. Katayama, T. Nagai, H. Taniguchi, K. Satoh, N. Tajima and R. Kato, to be published in *J. Low Temp. Phys.* (2006).
- [29] T. Lofwander and M. Fogelstrom: *Phys. Rev. Lett.* **95** (2005) 107006.
- [30] K. Yamada: *Electron Correlation in Metals* (Cambridge Univ. Press 2004).
- [31] H. Kontani and M. Ohno: *Phys. Rev. B* **74**, 014406 (2006).